

2012

Modeling of Tooling-Workpiece Interactions on Random Surfaces

Hitesh Kataria

Andres L. Carrano

Brian K. Thorn

Follow this and additional works at: <https://digitalcommons.fairfield.edu/engineering-facultypubs>

Copyright © 2012 Hitesh Kataria et al. This is an open access article distributed under the Creative Commons Attribution License, which permits unrestricted use, distribution, and reproduction in any medium, provided the original work is properly cited.

Peer Reviewed

Published Citation

Kataria, Hitesh, Andres L. Carrano, and Brian K. Thorn. "Modeling of Tooling-Workpiece Interactions on Random Surfaces." *Advances in Mechanical Engineering*, (January 2012). <https://doi.org/10.1155/2012/807018>.

This item has been accepted for inclusion in DigitalCommons@Fairfield by an authorized administrator of DigitalCommons@Fairfield. It is brought to you by DigitalCommons@Fairfield with permission from the rights-holder(s) and is protected by copyright and/or related rights. **You are free to use this item in any way that is permitted by the copyright and related rights legislation that applies to your use. For other uses, you need to obtain permission from the rights-holder(s) directly, unless additional rights are indicated by a Creative Commons license in the record and/or on the work itself.** For more information, please contact digitalcommons@fairfield.edu.

Research Article

Modeling of Tooling-Workpiece Interactions on Random Surfaces

Hitesh Kataria, Andres L. Carrano, and Brian K. Thorn

Kate Gleason College of Engineering, Rochester Institute of Technology, 81 Lomb Memorial Drive, Rochester, NY 14623-5603, USA

Correspondence should be addressed to Andres L. Carrano, alceie@rit.edu

Received 8 March 2012; Accepted 6 August 2012

Academic Editor: Yung C. Shin

Copyright © 2012 Hitesh Kataria et al. This is an open access article distributed under the Creative Commons Attribution License, which permits unrestricted use, distribution, and reproduction in any medium, provided the original work is properly cited.

Abrasive processes, commonly employed in manufacturing, are difficult to model because they rely on brittle particles with unknown geometry and multiple points of contact. Newly developed microreplicated abrasives allow for control of abrasive grit properties such as size, shape, and distribution. This paper proposes and validates a parametric model of abrasive machining that allows for studying the interaction of this particular tooling with randomly generated surfaces. In this work, the parameters of a probability distribution function that represents the workpiece surface are approximated by profilometry data. Monte Carlo simulation is used to account for inter- and intraspecimen variability. A geometric representation is used to mathematically represent the interaction between workpiece and tool. The results show good correlation between theoretical and actual values. This approach could be used to aid in tool geometry design as well as in process parameter optimization.

1. Introduction

Most parts rarely obtain their final finish through manufacturing processes such as casting, forging, or machining. Secondary processes such as grinding, sanding, and polishing are typically used to impart the workpiece with its final surface quality. These abrasive machining processes rely on tooling that is highly variable with respect to particle size, distribution and density of the abrasive grits. Also, the orientation of the grits varies between tools and within the same belt of grinding wheel. This is mainly due to the nature of the process involved in manufacturing coated abrasives, whereby multiple layers of oriented grits of approximately the same size are attached to a substrate and further oriented with gravity or electrode-induced polarization. Consequently, it is not surprising that abrasive-based machining processes have been among the most challenging to accurately model and characterize.

Early modeling efforts have addressed this area by assuming specific tooling and workpiece conditions. Several researchers [1–4] have adopted a “single-grit” approach. These studies model the interaction between a single-point abrasive tool and a workpiece in a deterministic way. Extensions of this approach have produced contributions with respect to the ploughing phenomenon and elastic-plastic

effects [3, 5]. Williams and Xie [6] developed a three-dimensional model that predicts the tangential force between a pyramidal asperity and a ductile surface. This work also investigates the interaction of several abrasive passes on wear tracks while determining the importance of the distance between tracks upon wear mode. Other efforts [7] have investigated the interaction between a geometric computer tool model on a perfectly flat surface. Bouzakis and Karachaliou [8] developed a computer model that uses the wheel cutting profiles to determine the chip geometry in the cutting edge of each grain. A different approach suggests modeling the variability in particle size, shape, and placement in the substrate by assuming statistical distributions [6, 9–11]. This stochastic approach is useful for developing input-output correlations that are the basis for predictive process capabilities. Sayles and Thomas [12] found that the initial height distribution of a grinding wheel is negatively skewed, but also that it will approach a Gaussian distribution with further grinding. The work by Jiang et al. [11] considers wear rate and size effect for multiple conical particles with round tips. However, the common gaps found in these studies include (i) the interaction between multiple layers and rows of abrasive grits has been studied in a limited way and; (ii) the initial condition of the workpiece surface (i.e., surface roughness) is usually not considered as an input.

In addition, technological innovations on the manufacturing processes of abrasives have allowed for precise location of the abrasive grits on the substrate. This technology, called microreplication, consists of precise casting of three-dimensional structures (such as pyramids or cones) onto a backing material (Figure 1). When compared to traditional coated abrasives, these structured abrasive tools are more deterministic with regards to shape, size, distribution, and orientation of the grits.

The objective of this study is to develop and validate a parametric model of the engineered abrasives that allows studying the interaction of this particular tooling with various random surfaces. This would allow prediction of surface roughness from a given tool-workpiece pair as well as determining the appropriate tool geometry and process parameters for a specific application.

2. Materials and Methods

This work has been subdivided into four areas: (i) parametric modeling of abrasive tooling, (ii) generation of random workpiece surfaces, (iii) modeling of tool-workpiece interactions, and (iv) experimental validation.

The purpose of the first effort is to develop a computer model flexible enough to define, manipulate, and visualize the different geometric parameters of the tooling. The parameters of interest are the size, shape, and distribution of the abrasive grits as well as their relative orientation with respect to the feed direction. Since it is the predominant commercially available configuration, this study focuses only on pyramid-shaped grits with a rectangular base. The second effort seeks to develop a model capable of representing different random surfaces with the same profile roughness distribution prior to machining. Reverse metrology from specimens is used to obtain data and fit a probability distribution with its respective parameters. Random surfaces are then generated from these distributions. The third effort combines the earlier two outputs to model the interaction and produce the resulting surfaces. A graphical representation of this interaction is generated along with the assessment of the resultant profile after machining. All the computational models for the tool, workpiece, and tool-workpiece interaction were developed in Matlab. The final effort is directed towards validating the model with experimental data.

3. Parametric Modeling of Abrasive Tooling

One of the most commonly available engineered abrasives possesses pyramid-shaped grits with rectangular bases. The proposed tooling model is generated by characterizing and varying the geometric parameters such as the base widths, height, and the pattern of these pyramidal shaped abrasive grits.

The dimensions of the geometric parameters that are used as input to develop the tooling model were extracted from a micrograph of an actual abrasive sheet. Using image analysis software, base widths of the pyramid-shaped tool

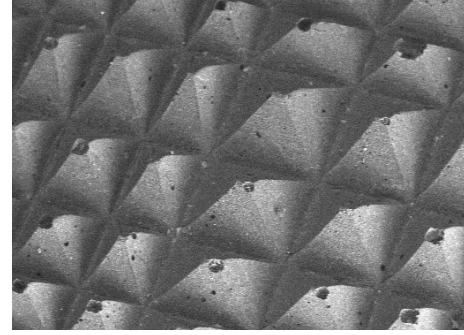


FIGURE 1: SEM micrograph of structured abrasives (20.0 kV).

were measured and mapped into a computer representation (Figure 2). The tool model representation shown in Figure 2 is a 4×7 patch of pyramidal grits generated in Matlab. Two-scaling vectors characterize the deviations of each base width with respect to a predefined nominal square. This patch is the fundamental area to be replicated by the computer model several times across and along to form the virtual belt, thus imitating the manufacturing conditions that produced the tooling. The extent of the abrasive area can then be defined by determining the number of patches to be replicated, as well as by manipulating the scaling vector of the overall size of the patch.

It is also necessary to state the angles which these grits would have with respect to the feed direction (constrained along the Y axis in this model). This is determined by the *attack angle* α (Figure 3) which can be thought of as the take-off angle from the edge of the abrasive belt. The attack angle is used as an input to homogeneous transformation matrices to rotate the patch of pyramids about the Z axis

Every square in Figure 3 represents the projection onto the X - Y plane (top view) of a four-sided pyramidal grit. This can be specified in the model by selecting the number of grits per row (N), any number of total rows (M), and the base widths (a_1 and a_2). By selecting the appropriate pyramid height (h), it is then possible to completely define the pyramidal geometry. The rake angle is given by the parameters (a_1 , a_2 , and h) along with the orientation of the pyramid with respect to the feed direction (α). For a square-based pyramidal grit of length a , the rake angle is contained in the interval depicted by

$$\text{Rake Angle} \in \left[-\arctan\left(\frac{a}{2h}\right), -\arctan\left(\frac{a\sqrt{2}}{2h}\right) \right]. \quad (1)$$

At this point, it is possible to obtain a 3D graphical representation of the grits (Figure 4). In this example, the configuration is one patch of 7 grits per row, 4 rows, and 35° attack angle. From Figure 4, it can be noticed that projections of the grit matrix onto planes XY and XZ are calculated and plotted. The projection onto plane XY is developed for visualization purposes while the projection onto plane XZ is the foundation for obtaining the cumulative 2D tooling profile that would later be used to interact with the workpiece. Because the model of the abrasive matrix has a finite

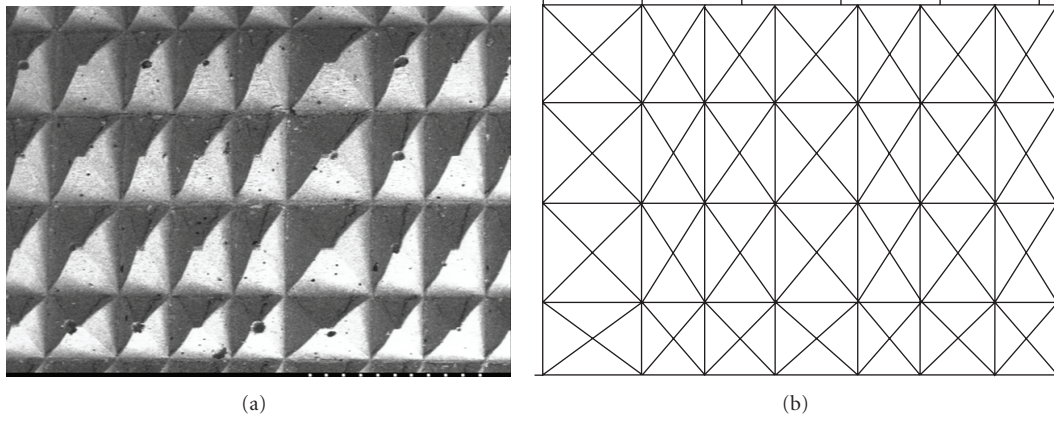


FIGURE 2: Tool model representation of pyramidal grits.

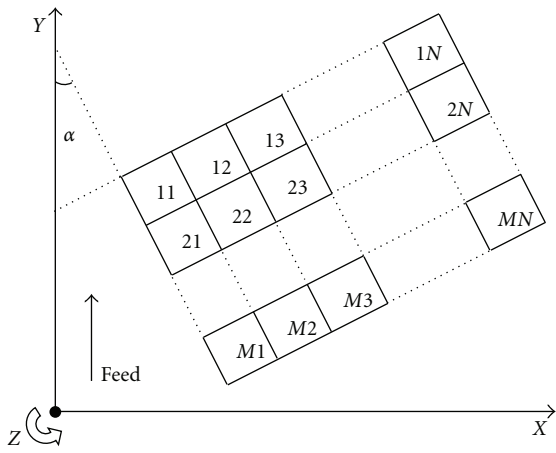


FIGURE 3: Two-dimensional representation of tooling matrix.

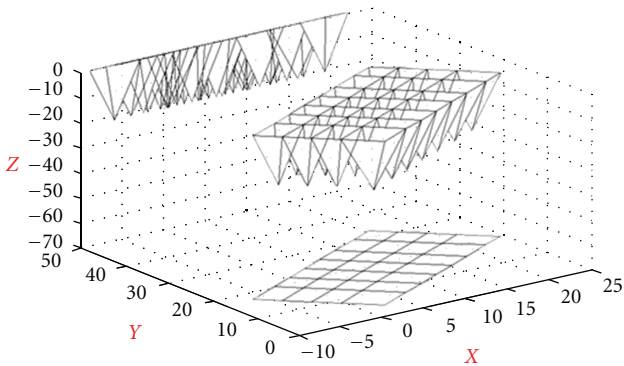


FIGURE 4: Isometric view of tooling matrix.

size, only the region that is swept by all rows of grits is considered for analysis.

4. Generation of Random Work Surfaces

The next step after developing a model of the tooling was to represent the profile of the work surface. The underlying

idea was to use reverse metrology to obtain the discrete and summary information of the roughness profile of actual surface specimens prior to machining. This information, in turn, was used to estimate the parameters of a probability distribution for further generation of random surfaces. This allowed for generation of multiple surfaces from identical profile distributions, thus accounting for the inherent random variability of the surfaces as well as the limitations of the measurement process. Figure 5 describes the surface generation process. Stylus-probe profilometry as well as light interferometry was used to collect the surface descriptors root mean square roughness (R_q) and profile skewness (R_{sk}) [13].

These surface descriptors were used to estimate the parameters of a gamma distribution. The surface parameters R_q (root mean square roughness) and R_{sk} (skewness of the profile) are calculated according to the ASME B46.1 standard [13], as shown in

$$R_q = \left[\left(\frac{1}{L} \right) \int_0^L Z(x)^2 dx \right]^{1/2}, \tag{2}$$

$$R_{sk} = \frac{1}{R_q^3} \frac{1}{L} \int_0^L Z^3(x) dx,$$

where Z represents the height deviations taken within the evaluation length (L) and measured from the mean line.

The probability density function of a gamma distribution can be described by two parameters as shown in

$$f(x) = \left(\frac{x}{b} \right)^{c-1} \frac{e^{-(x/b)}}{b\Gamma(c)}, \tag{3}$$

where b is the scale parameter and c is the shape parameter ($b > 0$ and $c > 0$). For the model in this paper, the suggested approach is to approximate the values of the shape and scale parameters by using summary data from surface scans. Since the variance of the gamma distribution is given by the expression shown in

$$\text{Variance} = cb^2, \tag{4}$$

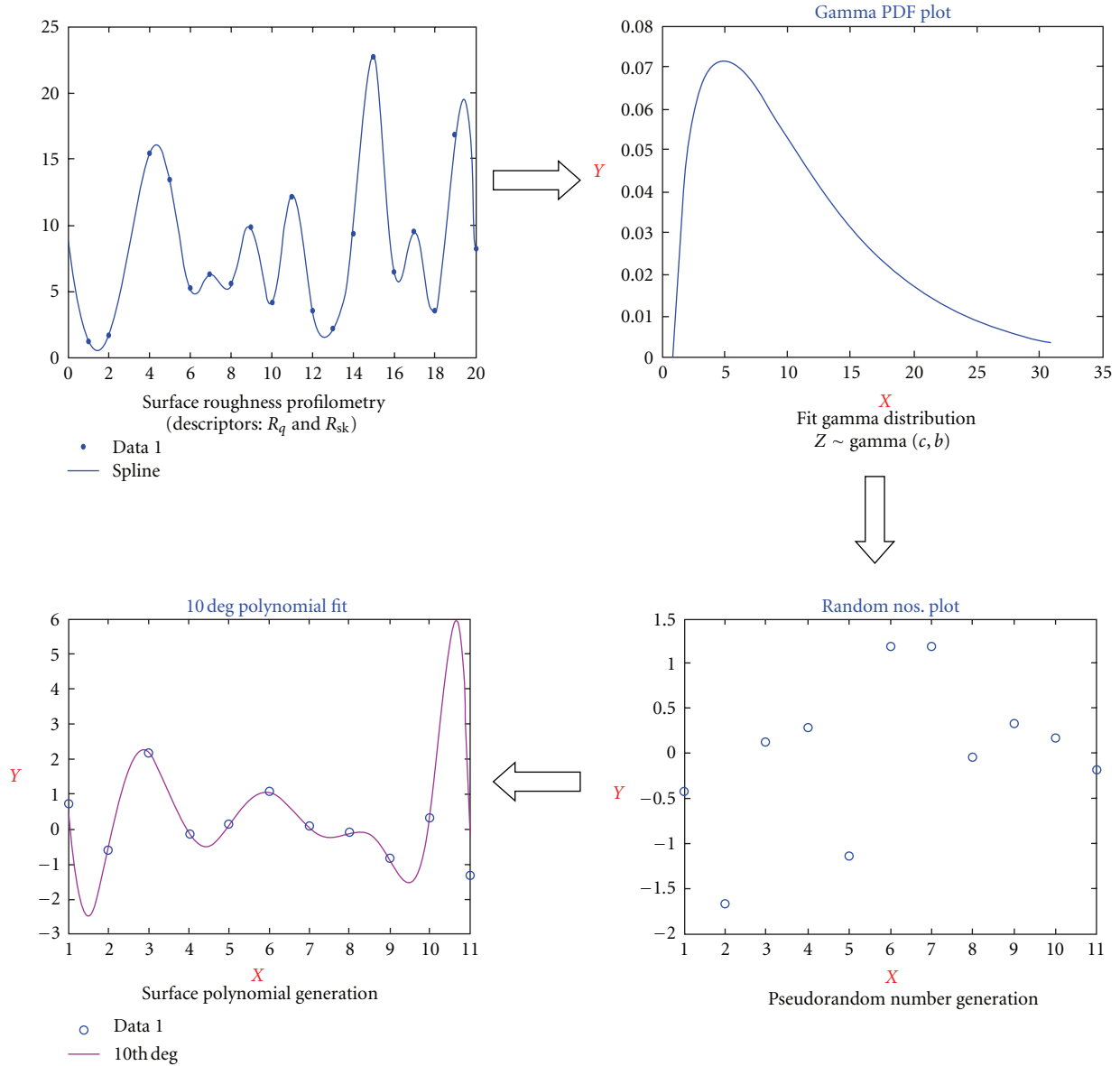


FIGURE 5: Generation of random work surfaces.

it is then proposed that the scale parameter can be calculated by approximating the variance by the root mean square (rms) average roughness obtained from the surface, as shown in

$$b = \frac{R_q}{\sqrt{c}}. \quad (5)$$

Similarly, the skewness of the gamma distribution is given by

$$\text{skewness} = \frac{2}{\sqrt{c}}. \quad (6)$$

The shape parameter is then calculated by approximating skewness of the distribution by the skewness of the profile obtained from the surface scanning. This is shown in (7).

$$c = \frac{4}{R_{sk}^2}. \quad (7)$$

This process creates a distribution from which it is possible to generate pseudorandom points to fit new surfaces, which is suitable for a Monte Carlo simulation scenario. This random generation of surfaces allows for the incorporation of variability into the workpiece surface model while maintaining the average surface descriptors of the native surface.

The randomly generated sets of numbers are used to characterize the surface by fitting a 15-degree polynomial. The degree of the polynomial was chosen to be one of the largest that did not exhibit the edge oscillations known as the Runge phenomenon. Since the roughness data is typically presented in equidistant nodes, a polynomial interpolation greater than 20 degrees would cause severe oscillations at the edges of the interval, thus increasing the interpolation error. These oscillations can be minimized by using Chebyshev's nodes instead of equidistant ones or simply by increasing

the density of the points towards the edges of the interval. Each generated random surface is then rotated via homogeneous transformations, projected in the XZ plane, and superimposed with the 2D-pyramid grits tool projection. The workpiece and tool are now projected in the same plane and their interaction can now be modeled, thus emulating the machining process.

5. Modeling of Tool-Workpiece Interactions

The first step in modeling this interaction was to develop an equation describing the amount of tool indentation as a function of the applied load. This was empirically obtained by performing controlled Vickers (pyramidal indenter) hardness tests on the material of interest and subsequently developing the load-indentation relationship. Afterwards, it was necessary to obtain the polynomial equation representing the work surface as well as the line equations from the abrasive tooling profile that were relevant. The latter consisted of the line equations for the edges of each grit that were boundaries in the XZ tool-workpiece projection. Finally, to obtain the surface profile left in the workpiece after M passes, it was necessary to calculate the intersection points between relevant surface profile and tool projections.

Since the relevant edges of the pyramid grits are represented by line equations and the surface by a polynomial equation, the intersection points can be obtained by numerical methods. In this work, a Newton-Raphson approach was used to approximate the relative roots of the surface polynomial with respect to the tooling edges. A compensation algorithm was developed and introduced to alleviate approximation errors. This process yields a point cloud that, once connected, depicts the resulting surface after machining. The machined profile is shown in Figure 6.

The assessment of the resulting profile was developed to resemble that of a profilometer. In order to calculate surface descriptors, the machined profile is scanned at a user-specified sampling length and the points stored in a database for surface descriptor calculation. For this study, the following surface roughness descriptors were assessed: average profile roughness (R_a), root mean square roughness (R_q), maximum profile valley depth (R_v), maximum profile peak height (R_p), and maximum peak to valley (R_t) as well as profile skewness (R_{sk}) and kurtosis (R_{ku}).

6. Experimental Validation

For the purpose of model validation, a customized experimental apparatus was constructed and aluminum specimens were prepared. The abrasive tooling consisted of an engineered abrasive belt that is commercially available. The attack angle on these belts is 35° . The verification experiments included machining polished aluminum samples with strips cut out from the belts and under controlled loads. The two attack angles considered in this study were 0° and 35° as they were the two configurations most easily measured and setup with minimal error. Once the tooling was setup in position, the attack angle was verified by applying ink to the grits

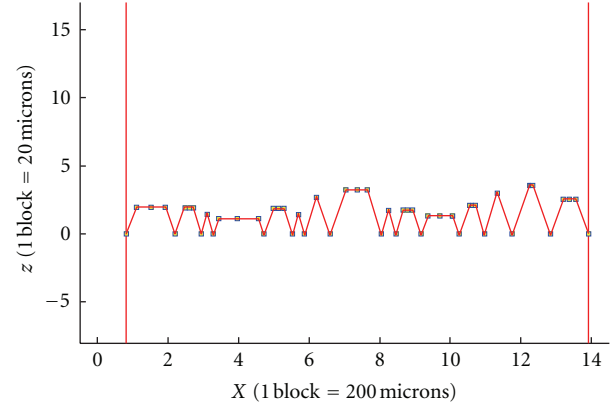


FIGURE 6: Model of a machined profile.

and pressing the belt against paper. The idea was then to produce samples at these two angles and for identical loads and number of passes and subsequently compare the trends from this experiment with those obtained from the model. A phase-shift interferometric microscope (wavelength 550 nm) was used to assess the surface topography and descriptors.

The testing apparatus (abrader) was custom designed and built. It was intended to hold a specimen in position while a controlled load was applied over a known area. It also had to be stiff enough to withstand the dynamics of an abrasive strip sliding between the workpiece and the lever mechanism with minimal lateral movement. The device consisted of a lever mechanism with a titanium shoe that pivots about a shaft. This allowed a more localized pressure and easier calculation of the area of contact. The specimens were mounted on a manually driven microstage. The area of contact was measured and found to be 1.16 cm^2 . There were six steel weights available for a combined total weight of 1350 grams. An abrasive strip was pulled at a constant speed to generate the abraded surface. Figure 7 shows a picture of this apparatus.

The specimen preparation involved machining of aluminum 2024-T351 bar stock down to a specimen size of $1'' \times 1.75'' \times 0.75''$ and prepared into the smoothest possible surface. Twelve specimens were cut and faced with a shell endmill in a vertical machining center. Following this, the specimens were run through a sequence of two grit sizes (P-1200 and P-2500) in a bench belt grinder and then processed in a polishing wheel with a $6 \mu\text{m}$ diamond paste thinned with a Buehler paste extender. This was followed by a polishing operation in a wheel with $1 \mu\text{m}$ Al_2O_3 slurry. This preparation sequence produced a near-mirror finish on all specimens.

A correlation between the load applied and the indentation amount was developed for the material of interest. This was accomplished by a series of controlled Vickers microhardness tests with a 136° diamond indenter. The microhardness experiment showed a very linear relationship between the load applied and the depth of penetration between 50 and 1350 grams. Since the pyramid angle in the Vickers indenter is slightly different from that in the abrasive grit, this

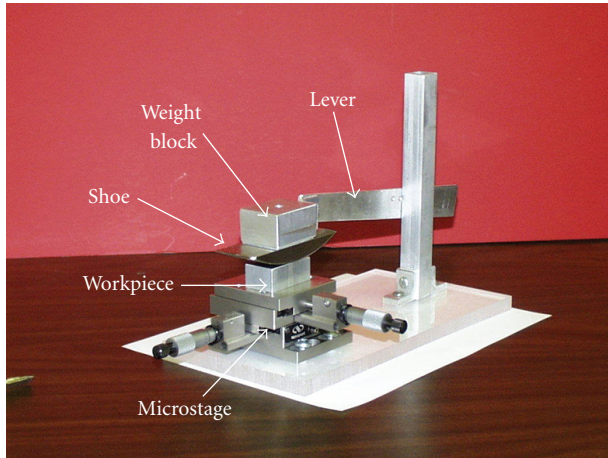


FIGURE 7: Abrader apparatus.

approximation had to be based on the assumption of equal energy required for displacing dislocations in the material by both pyramidal indenters. Also, in order to incorporate the depth of indentation into the model, another important assumption had to be made. It was assumed that the strain fields originated during abrasion were similar to those from the indentation experiment. Finally, the abrasive tooling utilized was silicon carbide A-110 (equivalent to a P180 FEPA).

Scanning electron microscopy was utilized for performing reverse metrology on the pyramids and for illustration purposes. The metrology for base width was performed by processing a nontilted image with measurement software. The average measurements from 28 pyramids yielded an average base of $843 \mu\text{m}$ and pyramid height of approximately $415 \mu\text{m}$. This yielded a base-height ratio of approximately 2:1.

7. Results and Discussion

The model was run a total of 10,000 iterations. The configuration of the model was a grit matrix of 6×10 , with base widths following a uniform distribution between 630 and $1000 \mu\text{m}$. The virtual sampling length was set at $0.05 \mu\text{m}$, while the indentation depth at $34 \mu\text{m}$. Two attack angles were compared: 0° and 35° . Surface assessment on the actual specimens was performed before and after machining with a phase-shift interferometric microscope (wavelength 550 nm). The area of sampling was $500 \mu\text{m} \times 500 \mu\text{m}$. The starting roughness (R_a) for the polished specimens was measured at $0.032 \mu\text{m}$. The results are summarized in Table 1.

As seen in Table 1, the results obtained from the computer model correlate relatively well with those obtained with the instrumentation on the actual surfaces, especially at 35° attack angle. However, the model underestimates the R_a roughness descriptor at 0° by 21%. Although this is a reasonable departure when modeling abrasive processes, the most probable explanation is related to the orientation of the grits. When machining at 0° attack angles, the grits line up parallel to the feed direction, superimposing their projections, thus

TABLE 1: Experimental and computer model results (values are R_a in μm).

	Profilometry (actual specimens)	Computer model (predicted—average of 10,000)
0°	3.36	2.65
35°	3.38	3.39

creating fewer valleys in the surface. If the discrete virtual scanning misses such valleys, then a readout characteristic of a smoother surface will result. Although more general, other explanations for such discrepancies include the following.

- (i) The abrasive process is sensitive to wear and fracture, especially during the break-in phase of new abrasives. This would likely cause a change in geometry.
- (ii) Mechanical and physical properties of the material are not necessarily homogeneous and may vary due to localized effects (e.g., residual stresses, hard spots, etc.).
- (iii) The material removal mechanisms are not 100% efficient. It has been reported [14, 15] that approximately 15% of the groove volume is removed to form a chip and that the remainder forms ridges on the metal surfaces. The model assumes 100% material removal and thus could lead to discrepancies in final results.
- (iv) The relative bluntness of nonideally sharp tip decreases with increasing penetration depth.

Further understanding of the individual effects of the parameters in the model (abrasive size, pyramid height, indentation depth, and attack angle) can be obtained by applying the model. Figures 8 and 9 depict the main effects of the abrasive matrix size and attack angle, respectively.

Figure 8 indicates that the number of pyramid grits, a surrogate of machining time, presents a substantial influence on the surface roughness. Initially, as the size of the abrasive is increased, the surface descriptors R_a , R_q , and R_t experience a decrease of as much as 57%. This behavior is expected and is the main reason for which abrasive operations are employed for surface finishing. The decrease in value of roughness descriptors, indicating a smoother surface, is due to the multiple pass effect: as the numbers of pyramids increases the number of grits interacting with the work piece also increases thus resulting in more material being removed. However, after certain abrasive size or, similarly, certain machining time, the surface roughness descriptors reach a plateau and no significant improvement is observed. This behavior is consistent with that reported in the literature [16], and its accurate characterization can be used to monitor abrasive use to optimally set machining times or cost-effective belt replacement policies.

With respect to the attack angle (Figure 9), the smooth roughness obtained at low attack angles ($\alpha < 10^\circ$) is the consequence of significant overlap of consecutive rows of

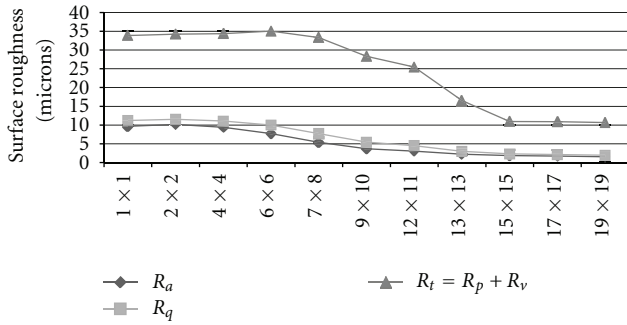


FIGURE 8: Main effect of the abrasive matrix size (number of grits per column and rows).

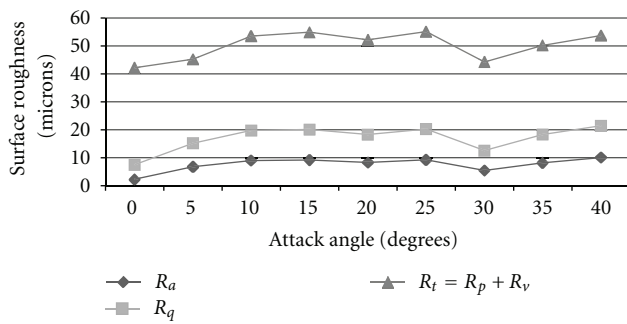


FIGURE 9: Main effect of attack angle.

abrasive grits. This causes large areas of highly polished ($R_a = 0.032 \mu\text{m}$) surface to be left untouched, thus producing a seemingly smoother finish. Once the attack angle is large enough to guarantee a complete coverage ($10^\circ \leq \alpha \leq 40^\circ$), the average roughness R_a behaves robustly between 50 and $55 \mu\text{m}$. The exception is the 30° configuration which presents a significant drop in all roughness descriptors. This shows the potential of this method for assisting in tool geometry design; in this example the 30° configuration would be the preferred manufacturing target over the current commercial configuration (35°).

Finally, the main effect of indentation depth, a surrogate of pressure, showed an initial linear increase but the descriptors quickly reached a plateau and stabilized. The initial increase in the descriptors can be explained by the fact that, initially, for small indentation depths, the grits are barely scratching the surface. This leaves untouched areas, which is obviously undesired, but roughness is low because the initial surface was highly polished. The reason can be geometrically described as having all the intersection points between the projections of different grits taking place above the surface level. On the other end, and after reaching a certain level of indentation, further pressure did not result in a better surface (as all the intersection points were already below the surface level and additional pressure did not generate any new surface profiles). This is consistent with the findings of Taylor et al. [17] in which the surface roughness did not improve when increasing the interface pressure after all grits were fully engaged.

8. Conclusions and Future Work

In this work, a parametric model of multiple-pass abrasive machining that employs reverse metrology as well as statistical and numerical methods is proposed and validated. The theoretical values correlate well with the actual readings. The model is flexed to analyze the individual effects of certain tool and process characteristics. The method shows potential for aiding in tool geometry design or process parameter optimization. Implementation of this model could lead into specific grit orientations on the substrate (belt or wheel) or grit characteristics (i.e., height or width) that would yield either the best surface quality (or a specific target surface roughness) or that would simply perform more robustly under specific process conditions. Also, the model could aid in determining process settings (such as pressure, machining time, etc.) that would allow optimization of abrasive life, process cycle time, and so forth. Finally, this model could be used to explore other geometrical shapes for the abrasives (e.g., cones, truncated cones/pyramids) and support design of customized abrasives for specific applications. Future work will focus on exhaustive validation of this model under additional conditions (i.e., loads, different materials, different tool geometries, etc.). Also, since this model focuses only on height variation aspects of the workpiece surface, future extensions should consider frequency (e.g., spectrum of wavelengths, etc.) and slope aspects of the resulting surface.

Nomenclature

- a_i : Base widths of a pyramidal grit
- b : Scale parameter of the gamma distribution
- c : Shape parameter of the gamma distribution
- h : Height of a pyramidal grit
- L : Evaluation length of roughness profile
- M : Total number of rows (tooling matrix)
- N : Number of grits per row (tooling matrix)
- R_a : Average profile roughness
- R_q : Root mean square (rms) profile roughness
- R_v : Maximum profile valley depth
- R_p : Maximum profile peak height
- R_t : Maximum peak to valley
- R_{sk} : Skewness of the roughness profile
- R_{ku} : Kurtosis of the roughness profile
- Z_i : Height deviations with respect to mean line of roughness profile.

Greek Letters

- α : Attack angle (tool orientation with respect to feed direction)
- $\Gamma(x)$: Gamma function.

References

- [1] T. C. Butterly and M. S. Hamed, "Some factors affecting the efficiency of individual grits in simulated grinding experiments," *Wear*, vol. 44, no. 2, pp. 231–245, 1977.

- [2] D. A. Dornfeld, "Single grit simulation of the abrasive machining of wood," *Journal of Engineering for Industry*, vol. 103, no. 1, pp. 1–12, 1981.
- [3] M. Abebe and F. C. Appl, "Theoretical analysis of the basic mechanics of abrasive processes. Part II: model of the ploughing process," *Wear*, vol. 126, no. 3, pp. 267–283, 1988.
- [4] I. C. J. Lin, G. Sathyanarayanan, L. J. Plebani, and W. L. Buehler, "Analysis of single grit cutting of alumina," in *Proceedings of the 1996 ASME International Mechanical Engineering Congress and Exposition*, pp. 223–227, November 1996.
- [5] T. C. Buttery and M. S. Hamed, "Generation of random surfaces representative of abrasion," *Journal of Mechanical Engineering Science*, vol. 20, no. 3, pp. 133–141, 1978.
- [6] J. A. Williams and Y. Xie, "The generation of wear surfaces by the interaction of parallel grooves," *Wear*, vol. 155, no. 2, pp. 363–379, 1992.
- [7] A. L. Carrano and J. B. Taylor, "Geometric modeling of engineered abrasive processes," *Journal of Manufacturing Processes*, vol. 7, no. 1, pp. 17–27, 2005.
- [8] K. D. Bouzakis and C. Karachaliou, "Process models in grinding, based on a three dimensional description of the grinding wheel topomorphy," in *Proceedings of the 13th North American Manufacturing Research Conference (NAMRC '85)*, pp. 369–374, Berkeley, Calif, USA, 1985.
- [9] A. A. Torrance, "An approximate model of abrasive cutting," *Wear*, vol. 118, no. 2, pp. 217–232, 1987.
- [10] K. Li and T. W. Liao, "Modelling of ceramic grinding processes: part I. Number of cutting points and grinding forces per grit," *Journal of Materials Processing Technology*, vol. 65, no. 1–3, pp. 1–10, 1997.
- [11] J. Jiang, F. Sheng, and F. Ren, "Modelling of two-body abrasive wear under multiple contact conditions," *Wear*, vol. 217, no. 1, pp. 35–45, 1998.
- [12] R. S. Sayles and T. R. Thomas, "A stochastic explanation of some structural properties of a ground surface," *International Journal of Production Research*, vol. 14, no. 6, pp. 641–655, 1976.
- [13] ASME B46. 1, *Surface Texture: Surface Roughness, Waviness, and Lay: An American National Standard*, The American Society of Mechanical Engineers, New York, NY, USA, 1995.
- [14] R. Gåhlin and S. Jacobson, "The particle size effect in abrasion studied by controlled abrasive surfaces," *Wear*, vol. 224, no. 1, pp. 118–125, 1999.
- [15] J. Larsen-Badse, "Influence of grit diameter and specimen size on wear during sliding abrasion," *Wear*, vol. 12, no. 1, pp. 35–53, 1968.
- [16] A. L. Carrano, B. S. Vora, F. Sahin, and R. L. Lemaster, "Monitoring of abrasive loading for optimal belt cleaning or replacement," *Forest Products Journal*, vol. 57, no. 5, pp. 78–83, 2007.
- [17] J. B. Taylor, A. L. Carrano, and R. L. Lemaster, "Quantification of process parameters in a wood sanding operation," *Forest Products Journal*, vol. 49, no. 5, pp. 41–46, 1999.